ARTIFICIAL RESORT BEACH PROTECTED BY OFFSHORE BREAKWATERS AND GROINS

by

Shoji SATO and Norio TANAKA
Port and Harbour Research Institute, Ministry of Transport
1-1, 3-chome, Yokosuka, JAPAN

INTRODUCTION

In Japan, area of natural beaches has decreased in the vicinity of cities, towns and villages, in consequence of constructing ports and harbours, reclamating shore and beach, and building strom-surge prevention structures like sea dikes and sea walls. On the other hand, the demand of people for recreation area is increasing year by year with the improvement of living and economic conditions. Therefore, since several years ago, local governments have extensively been constructing artificial beaches and restoring eroded beaches on many places by the aid of the central government.

Such artificial beaches, however, need large amount of natural sand, in spite of the deterioration of sand supply and the soaring of sand price. Moreover, local governments are able to get subsidiary payments of the central government for the construction of artificial sand beach, but not for replenishing sand lost by wave action after the completion of the construction works. Therefore, most artificial beaches in Japan are usually protected by groins and offshore breakwaters in order to retain artificially filled sand. But in summer when sea is in calm condition, pollutant produced by sea-bathing people or discharged from the land is likely to stagnate in the vicinity of the shoreline on account of such structures.

From the above-mentioned, coastal engineering problems on construction and restoration of sand beach in Japan are:
(1) suitable arrangement of offshore breakwaters and groins from standpoint of artificial beach protection
(2) keeping the sea water of the beach clean
(3) estimation of profile change of the artificial beach due to wave action after its construction.
This paper presents the results of investigations conducted with the aim of solving the above coastal engineering problems related to artificial beach constructions at Suma and Ito beaches. The investigations are mainly conducted using model experiment.

SUMA BEACH

Natural Condition of Suma Beach

Suma Beach is located in the western portion of Kobe City along Osaka Bay as shown in Fig. 1. Fig. 1 shows a bathymetric map of Suma Coast surveyed just before the start of the construction of the

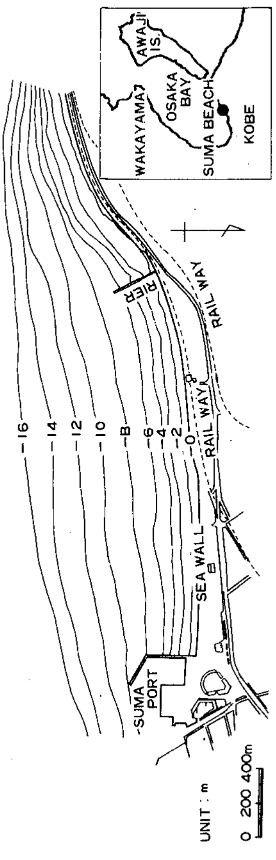

Fig. 1 Bathymetric map of Suma Coast

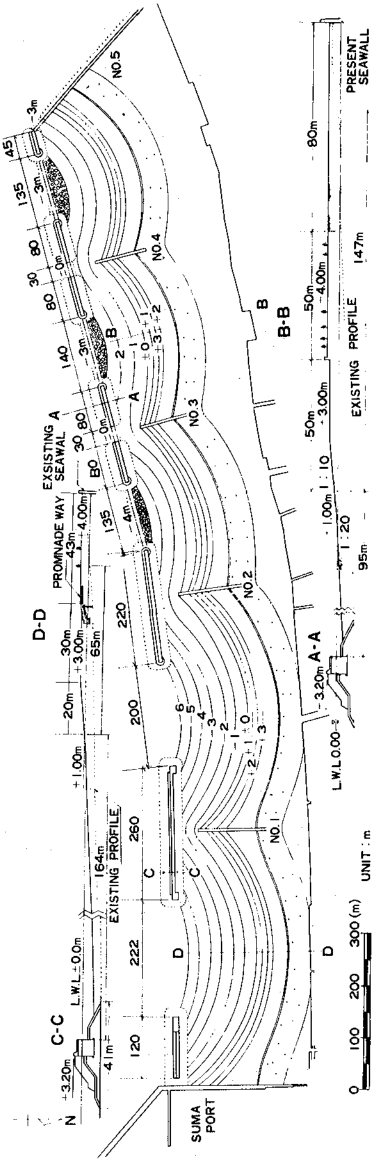

Fig. 2 The scheme of artificial beach at Suma of Kobe City

artificial beach, in 1973. The height of the backshore is 3 m above L.W.L., and the beach slope is nearly 1/10 on the foreshore and 1/20 - 1/30 between 1 and 6 m deep. The median diameter of the beach meterials are several mm on the foreshore and 0.3 to 0.5 mm between 1 and 6 m deep. Usually waves are so small and significant wave heights are less than 0.5 m. Waves of more than 1.5 m in $H_{1/3}$ come only a few time a year. But, in very rare cases, the beach is attacked by severe waves due to typhoons. The estimated past maximum $H_{1/3}$ is 4.75 m. Tidal currents are going and returning in parallel with the shore, showing maximum velocity of about 50 $cm.s^{-1}$ on the offshore of about 10 m deep at spring tide. The mean spring tidal range is 1.8 m.

Scheme of The Artificial Beach Construction

In 1973, Kobe municipal city has decided to construct the wide artificial beach on the stretch of about 2 km long between Suma Port, which is a leisure and fishery port, and the pier, which is a permeable type and is used to load materials for the reclamation of the area of Kobe Port. At that time, short groins of several ten meters long had existed on the whole stretch of the beach with space intervals of 100 m or so in order to prevent beach erosion, and behind the beach there was sea wall of 5 m high above L.W.L. in its crown height.

Fig. 2 shows the present scheme of the artificial beach designed on the basis of the model experiment which will be mentioned in the following paragraphs. The beach is devided into five parts by five long groins of No. 1 to 5, and there are six offshore breakwaters in order to protect the artificial beach from the wave action. The groins are of impermeable cellar type and the offshore breakwaters of composite type. The beach is filled with natural sand to form arch-shaped plane shape. The beach width, from the promnade way to the shoreline of mean water level, is about 50 m at the center of arch-shaped beach in the east portion. The green belt is behind the promnade way. In the west part of the stretch, the width of the coastal area is increased by the reclamation and the artificial beach is made in front of the reclaimed land, because houses denselyexist just behind it. Therefore, the width of artificial beach become so narrow that submerged rouble mound is constructed between the offshore breakwaters so as to retain the seaward end of the beach slope. The construction of the artificial beach began in 1973 and the most of the east portion in the figure will be completed in 1980 fiscal year.

Model Test on Sea Water Exchange in The East Part of The Beach

Model tests on sea-water exchange between inshore and offshore have been conducted using a fixed bed model with the reduced scale of 1/100 in both vertical and horizontal. Fig. 3 shows a pattern of the currents measured in the model of the east part of Suma Beach without the artificial beach, which corresponds to the state of the maximum of current velocity in flood tide at the site. There is a circulation of currents at the lee of the breakwater of Suma Port while the tidal currents in the offshore zone flow in pallalel with the shore line. Under the steady current with such flow pattern, the dispersion of fluorescent

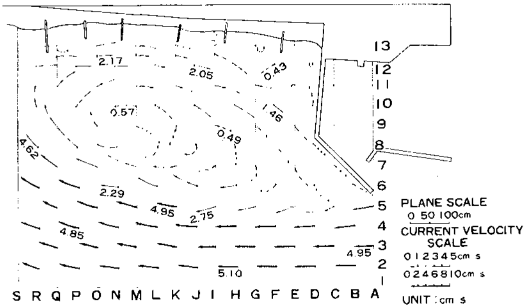

Fig. 3 Pattern of the fastest currents during flood tide at the east part of Suma Beach before the beach nourishment

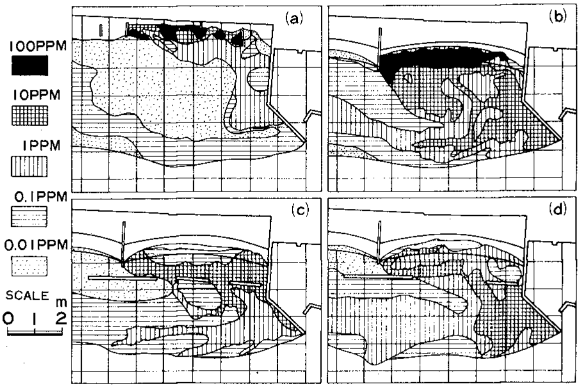

Fig. 4 Dispersion patterns of dye discharged on the shoreline in the east part of Suma Beach

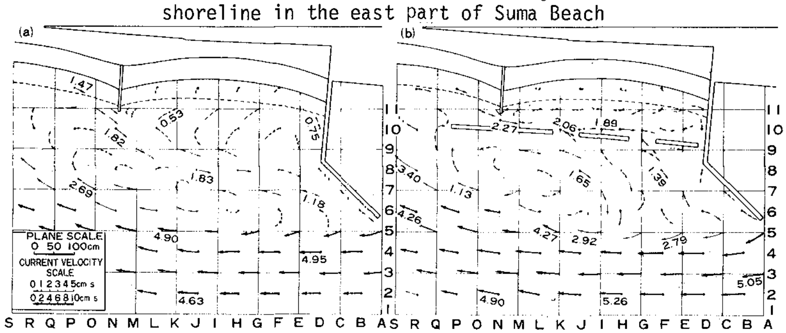

Fig. 5 Current patterns of the cases with and without offshore breakwaters

dye discharged on the shoreline has been investigated for cases with and without the artificial beach.

Fig. 4 shows the patterns of spreading dye at 60 minutes after the start of discharge of dye, though the dye of 500 ppm in density has been discharged only during the first 15 minutes at 8 points on the shoreline. The discharging rate is 0.222 cm^3s^{-1} per point. These diagrams were drawn by eyes on the base of colored pictures taken from the ceiling together with dye samples of 0.1, 1, 10 and 100 ppm in density placed on the edge of the model. In the figure, Case (b) of artificial beach with only groins is worse in offshoreward dispersion of dye than Case (a) without artificial beach, but Cases (c) and (d) with offshore breakwaters in addition to groins are better in it than the Case (a). It is because there are fast currents along the landward side of offshore breakwaters as well as circulating currents between offshore breakwaters and the shoreline at Cases (c) and (d), as seen from the patterns of currents shown in Fig. 5. The figure shows the result of test conducted under the same hydraulic condition as the above-mentioned Fig. 3. In comparison of Cases (c) and (d) in Fig. 4, the latter is better than the former. In these cases, the offshore breakwater is apart from the tip of the groin because it had been verified in the preliminary test that attaching them makes the water exchange worse between inshore and offshore.

Model Test on Beach Evolution in The Eastern Part of The Beach

Model tests on the beach evolution have been conducted using a movable bed model of 1/60 in vertical and horizontal scales. Fine sand of 0.19 mm in median diameter was used as sediments. Fig. 6 shows the comparison of depth contour lines before and after 6 hours run of waves of 4 cm in height and 1.03 s in period, which correspond respectively to 2.4 m and 8 s in the prototype on the basis of Froude's law. The direction of wave is south, and the still water level is equal to M.W.L. which is 1 m above L.W.L. in prototype. In the figure, the part of 1 to 3 m deep in the vicinity of the beach center is eroded by the wave action. The counter measures to prevent such erosion were tested under the same wave condition.

Fig. 7 shows the changes of the levels of the bottom between before and after 6 hours run of the same wave as Fig. 6 for each counter measure. Case 1 in the figure has a submerged breakwater of 3 m deep in crown level between offshore breakwaters, Case 2 it of 2 m deep in crown level on 6.5 m deep contour line, and Case 3 it of 2 m deep in crown level on 4.5 m deep contour line. In these cases having a submerged breakwater, the foreshore in the center of the arched beach erodes, and its backshore and the foreshore of both ends of the beach accrete. Case 3, which has a submerged breakwater in the nearest place to the foreshore, is the most elosive at the foreshore in the center of the arched beach. The submerged breakwater seems to be difficult to prevent the recession of the center part of the shoreline. Therefore, a small breakwater of 2 m above L.W.L. in crown level was placed in front of the foreshore, that is, on the 2 m deep contour lines. Its result is shown at (d) of the figure, where there are seen no erosion on the foreshore

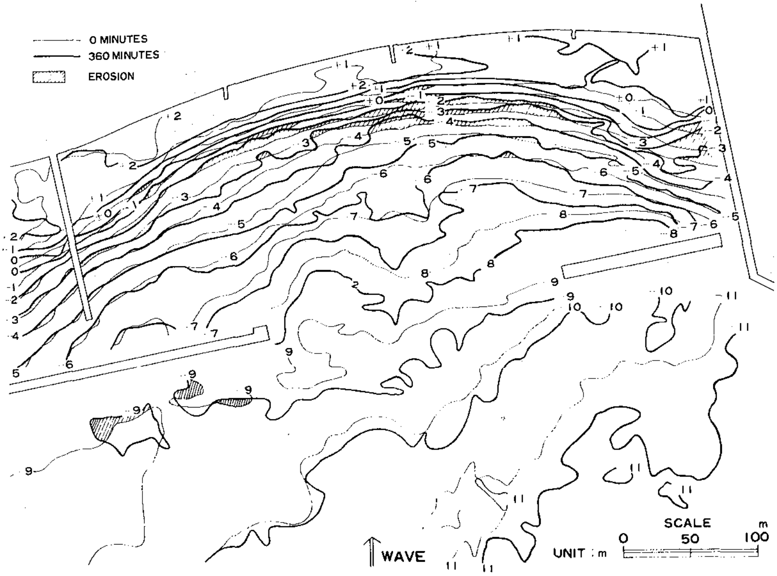

Fig. 6 Comparison of depth contour lines between before and after 6 hours wave action in the east part beach (H = 2.4 m, T = 8 sec)

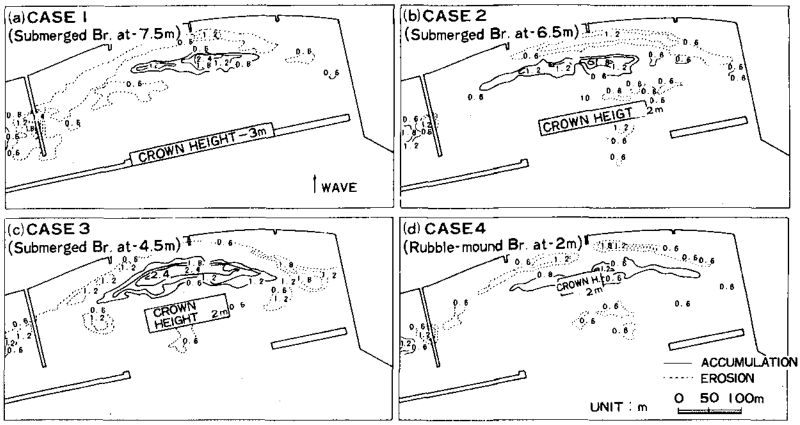

Fig. 7 Changes of the levels of bottom between before and after 6 hours wave action (H = 2.4 m, T = 8 sec)

just behind of the small breakwaters, though the areas around both tips of it are a little eroded.

Fig. 8 shows the change of bottom profile of the central part for each the above mentioned case. In every case except Case 4, the offshore side of shoreline is eroded by wave actions. This erosion is severer in the cases with a submerged breakwater than the case without any countermeasures. Therefore, Case 4 is recommended as the countermeasure against the recession of the center portion of the arched beach, but, at the site, the beach have been remained without any such a countermeasure at present. The reason is why such a structure is not welcomed from the view point of recreation and the model tests have a scale effect in their results. It will be again considered if such contourmeasure is necessary or not after finishing scheduled beach filling.

The Change of Bottom Topography in The East Part of The Beach

In the site, the beach filling was conducted every autumn from 1973 to 1977 at the east end portion, the total volume of filled sand being 180,000 m^3. Fig. 9 shows the changes of L.W.L. shoreline after the filling in September 1977, when 83,000 m^3 of sand was supplied so as to shift the foreshore seawards. The supplied sand was 1.6 mm in median diameter and 2.6 in Task's sorting coefficient. The shoreline of L.W.L, which was of nearly straight line, has receded in center and advanced in the both ends with the time. But, the latest change from December 1973 to June 1979 is very small, especially in the center part. It means that the shape of the shoreline has reached the state of equilibrium in nearly one year. This equilibrated shoreline is nearly simillar to that of the model test shown in Fig. 6.

Fig. 10 shows the changes of the beach profile at the center and the both sides of the beach. The profile of Section B at the center has changed mainly in the part above one meter deep, while these change appeared in the part above 3 m deep in the model test, as shown in the first section of Fig. 8. It seems to be because the most waves were less than 1.5 m in height at the site during the duration. The eroded sand in the center of the beach may have been transported along the foreshore to the both ends of the beach by the wave action. As the results, the foreshores of Section A and C have advanced and have become steeper than in the center portion. Despite such a bottom change, the total loss of filled material was only 2,500 m^3 in volume the period from September 1977 to March 1979.

Model Test on The Beach Evolution in The West Part of The Beach

The west part is, as described above, planned to be made in front of the reclamation land. The typical plane shape of artificial beach, which have been tested using a movable model of 1/80 in horizontal and 1/50 in vertical scale, are shown in Fig. 11. The three beaches are perfectly separated each other in Case 1 and are connected through the tip of the groin each other in Case 2 and 3. For each case, the crest level of the offshore breakwaters and the submerged breakwaters are 3.2 m above and 3 m below L.W.L., respectively. Moreover, Case 3 has the

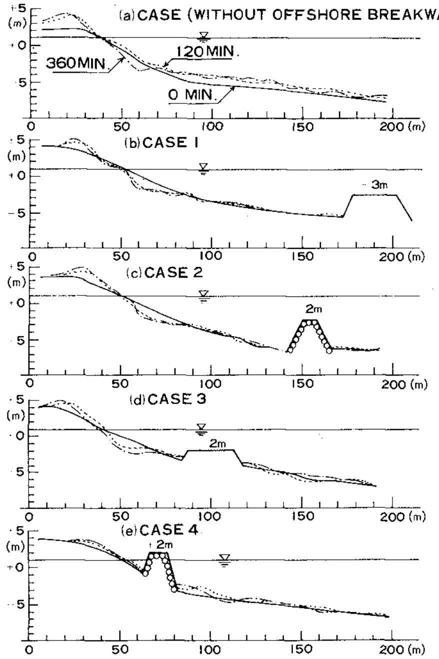

Fig. 8 Comparison of change of bottom profile along the central section

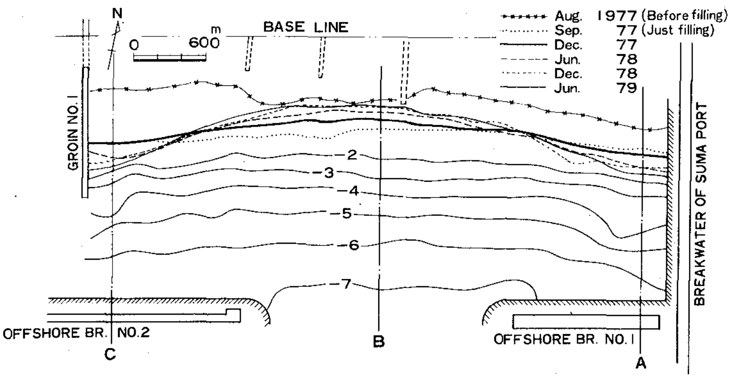

Fig. 9 Change of the shoreline of 10 m after the sand filling in Sep. 1977 at the site

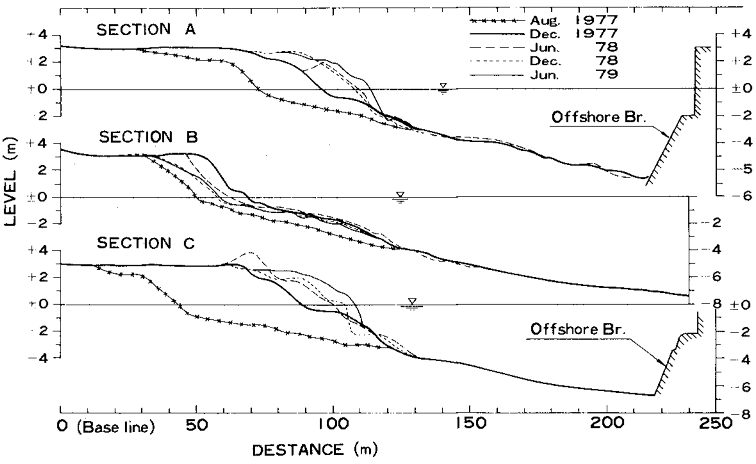

Fig. 10 Change of beach profile of the east part of the beach at the site

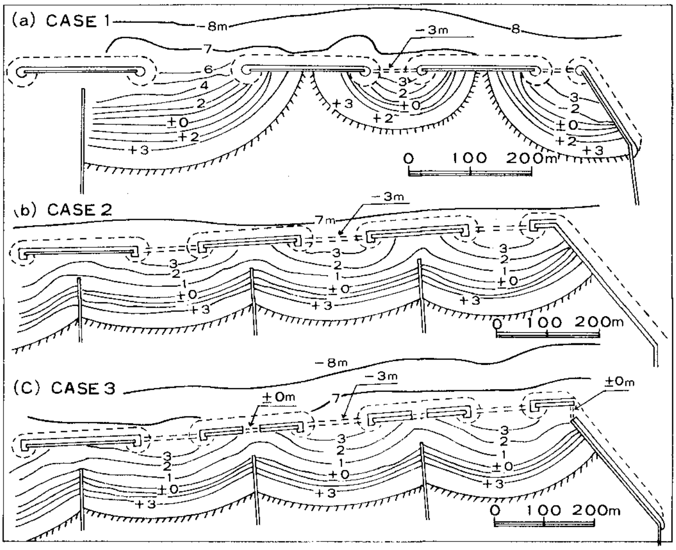

Fig. 11 Typical layouts of the artificial beach tested for the west portion

small open part of ±0 m deep in the center of the offshore breakwater. Fine sand of 0.29 mm in median dia. was used as sediments.

(a) Comparison between Cases 1 and 2

Fig. 12 shows the change of the water depth between before and after 6 hours run of waves of 5 cm in height and 0.85 s in period. The model waves correspond to the prototype waves of 2.5 m height and 6 s in period on the basis of Floude's law. The waves come from SSW and the bottom topography before the run is the same as that in Fig. 11. For both cases, each beach is eroded in the part directly facing the incident waves and accreted in its either side shetered by the offshore breakwaters. However, the quantity of water depth changes and the recession of shoreline at the center are severer in Case 1 than in Case 2 and more sand was lost seaward of the breakwater in the former case than in the latter case.

Fig. 13 shows the pattern of the currents caused by the waves for these two cases. The currents are measured by following by eyes the movement of a plastic ball of 0.7 cm in dia., the inside of which is filled with water so as for the ball to be a little heavier than the water. In Case 1, there are strong currents going outwards out of the open mouth of the western two beaches, but, in Case 2, there is not such current except weak currents in the central compartment. In Case 2, most currents approaching toward the offshore tip of either groin from the center of the beach flow towards the next compartment through the gap between the groin and the offshore breakwater. This difference of the current pattern is the cause that the sand loss in Case 1 is larger than that in Case 2. The seaward currents transport out the sands suspended on the beach by wave action.

(b) Comparison between Cases 2 and 3

Case 2 has rather large accumulation of sand in the vicinity of the tip of groin, as seen in Fig. 12. This accumulation is likely to grow up gradually and obstruct the current flowing toward the next compartment through the gap. Case 3 is a arrangement deviced to prevent such obstruction, having the small open part of ±0 m in its crown level in the center of the breakwater as mentioned previously. Fig. 14 shows the effect of the small open part, this is, the change of water depth between before and after 6 hours run of the same wave as (a) mentioned above but in SSE direction. In Case 3 with the small open parts, the vicinity of the tip of the groins is scoured and the recession of the shoreline at the center is smaller than in the Case 2.

The comparison of depth contour lines of the central compartment in these two cases is shown in Fig. 15 with the wave height ratio of Case 3 against Case 2. It is seen from the figure that the small open part makes wave height behind the offshore breakwater 3 - 1.5 times as large as the case without it, giving rise to currents running from it towards the base of the groin. As the results, the area around the tip of the groins is scoured and the accumulating area behind the offshore breakwater shifts toward the center of the compartment. Therefore, the sand transported along the shoreline from the central area of the compartment toward the both side decreases in volume, which prevent the recession of the shoreline at the center area of the compartment.

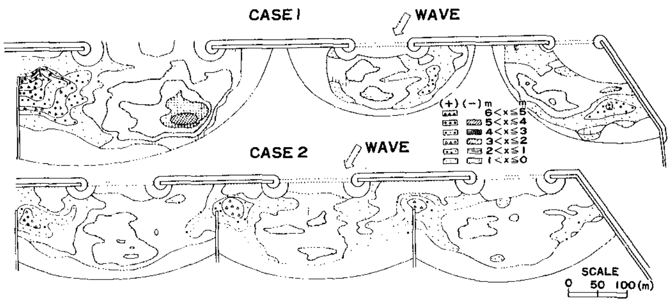

Fig. 12 Comparison of depth changes by wave action between Cases 1 and 2

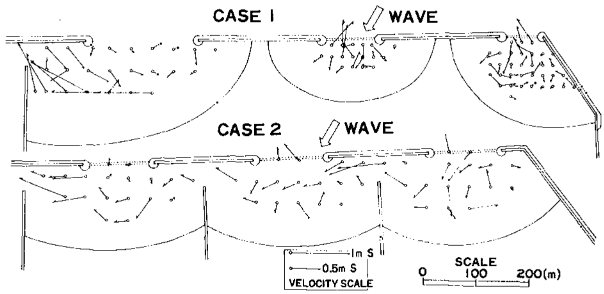

Fig. 13 Current patterns of Cases 1 and 2

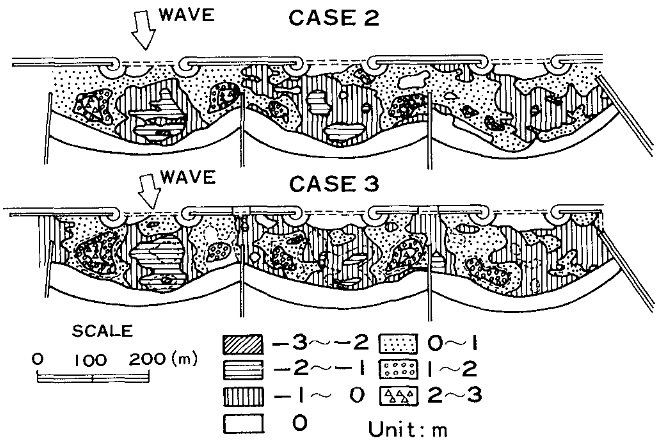

Fig. 14 Comparison of depth changes by wave action between Cases 2 and 3

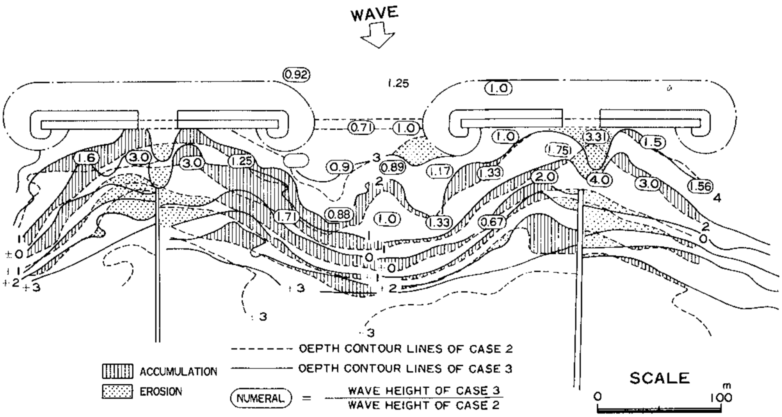

Fig. 15 Comparison of the depth contour lines between Cases 2 and 3

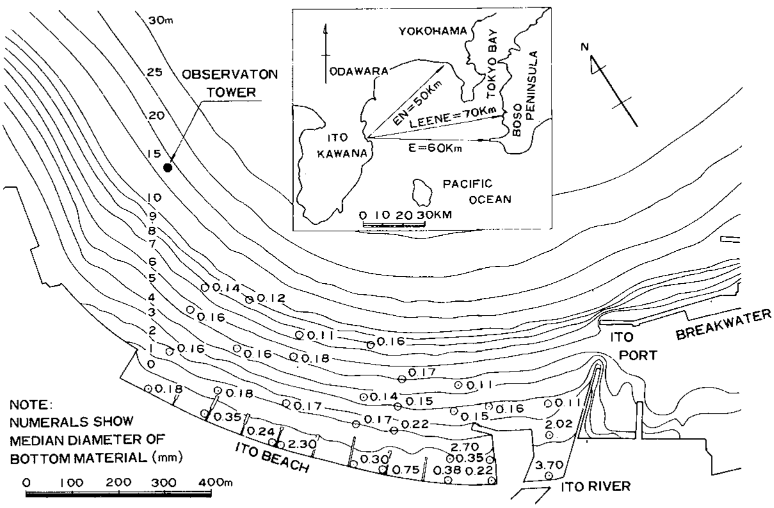

Fig. 16 Bathymetric map of Ito coast

ITO BEACH

Natural Condition of Ito Beach

Ito City is located at the east coast of Izu Peninsula which is about 100 km southwest from Tokyo as shown in Fig. 16. The figure shows bathymetric map of Ito Coast just before the beginning of the construction of the artificial beach, in 1973. The height of the backshore is 3 - 4 m above L.W.L. and the beach slope is nearly of 1/10 on the foreshore and 1/25 -1/30 between 1 and 6 m. But the deeper part than 10 m deep has steeper slope of about 1/10. The median diameter of sea-bed material is 0.2 - 0.5 mm on the foreshore and 0.2 - 0.12 mm on the offshore until 6 m deep.

The beach is sheltered by the head land of Kawana against southerly waves, as estimated from Fig. 16. Therefore, northerly waves are predominant at the beach, but their height is almost 1.5 m in H1/3 except when typhoons pass near the beach in summer and autumn. Tidal current flowing in nearly parallel with the coast in the offshore forms reverse circulating currents in the nearshore the velocity of which is weak and the order of several $cm \cdot s^{-1}$. The mean range of spring tide is nearly 1.5 m.

Scheme of Artificial Beach Construction

The beach of nearly 900 m long, which is to the west of Ito port as shown in Fig. 16, is at present protected by 8 groins of 40 - 60 m long and has the sea wall of 4.8 m above L.W.L. in crest height. The road just behind the sea wall is very jamed by traffic in resort season. Ito City, which is a tourist resort with hot springs, has decided in 1973 with the aid of the central government to change the beach into a more beautiful and cleaner resort place after widenning the road seaward by 7.5 m. Therefore, the authors have conducted the model experiment to make the plan of artificial beach.

Fig. 17 shows a plane view and a beach profile of the scheme of artificial beach which has been decided on the basis of the model experiment. A fishing basin of the east side and a slope way for fishery boats of the west side accommodate small fishery boats scattering on the beach at present. The present seawall is shifted seaward by 7.5 m as mentioned above, the green belt of 12.5 m wide is made, and artificial beach is arranged in front of the green belt. The beach is protected by three offshore breakwaters of 3.0 m above L.W.L. in crown height and three long groins, of which the two groins in the both side also work to protect the fishery boat area. The short wing parts parallel with the shore are attaching at the tip or its vicinity of each groin, which serves to stabilize sea-bed as shown later. The offshore breakwater are of rouble mound type covered with artificial brocks and the groin is of impermeable type of concrete blocks. Moreover, the tip part of each groin is protected with wave absorbers of artificial concrete blocks.

Model Test on Sea Water Exchange

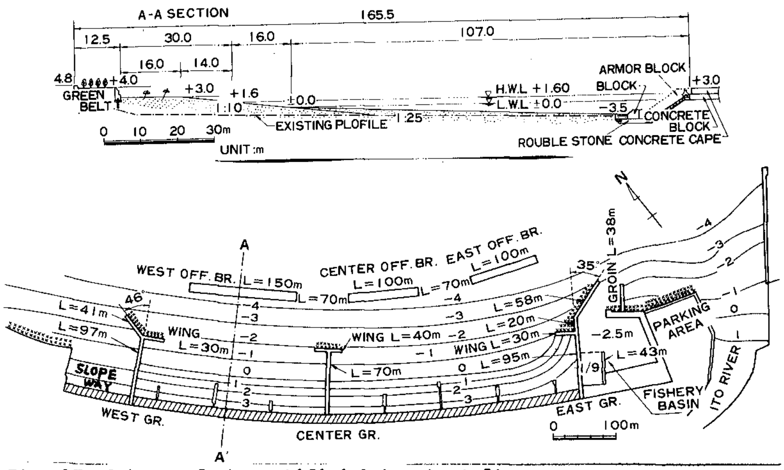

Fig. 17 Scheme of the artificial beach at Ito

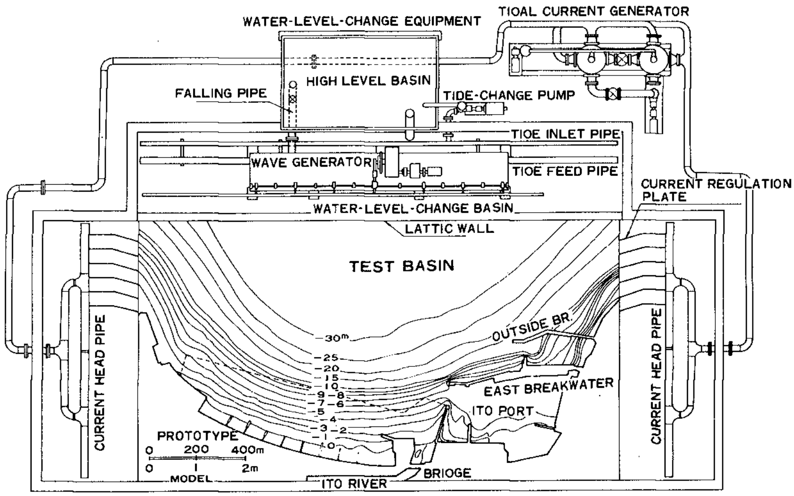

Fig. 18 A plane view of the model for sea-water exchange test

Fig. 18 shows a plane view of the model for the test on sea water exchange conducted in order to determine the above-mentioned scheme of Ito artificial beach. The model is of concrete mortar floor with the reduced scale of 1/200 in horizontal and 1/100 in vertical, in which the part deeper than 30 m deep blow L.W.L. is made as the constant depth of 30 m deep. A tidal current generator, of which the main part is shown in the right upper part of the figure, produces cyclic currents flowing from right to left or from left to right in the test basin by means of a pump and rotating valves. The water level in the basin is periodically changed by a water-level-change equipment, which pumps up some suitable volume of water from the water-level-change basin to the high-level basin together with falling down some water by gravity from the latter basin into the former basin through a falling pipe. The water-level-change basin is separated by a lattice wall from the test basin so that the water is able to commute between these two basin freely. A wave generator is arranged in the water-level-change basin so as not to disturbe currents in the test basin.

Fig. 19 shows the patterns of currents when both steady currents and waves are in force. The velocity of the steady currents corresponds to the maximum velocity of current at falling tide. The steady waves are 30 cm in height and 10 s in period which correspond to swells in summer. In the figure, numerals beside arrow marks of current direction show velocity in unit of $cm \cdot s^{-1}$. In (a) of the figure, there are reverse currents in the shallower area against the main currents flowing from left to right, and the currents of 10 $cm \cdot s^{-1}$ or so seen in the vicinity of the shoreline are caused by breaking waves. In (b) of the figure, there are comparatively strong currents flowing out from the open parts among offshore breakwaters and groins, though the current velocity inside the offshore breakwaters is nearly the same order as the existing state without offshore breakwaters and groins. The similar phenomenon appears also in the case of rising tide in which the main currents flow from right to left.

In order to check the influences of offshore breakwaters and groins on the sea water exchange between the onshore and offshore sides of these structures, fluorescent dye was discharged at 7 points on the M.W.L. shoreline only for 9 minutes at the time of the first H.W.L. and its dispersion was traced by taking the colour pictures from the ceiling under the condition that the sine curves of tide and current are generated to simulate the state of mean spring tide in addition to swells in summer. Discharged fluorescent dye is 700 cm^3 in volume and 500 ppm in density for each test. The current distribution at the M.W.L. of falling tide is the same as one shown in the above-mentioned Fig. 19. Fig. 21 shows the time changes of dye dispersion for the cases without and with the artificial beach, where each figure of 9 and 45 minutes corresponds to the first H.W.L. and the second H.W.L., respectively, as shown in Fig. 20. Currents flow from left to right in the offshore and from right to left in the nearshore during 9 minutes to 27 minutes. The dye discharged on the shore is transported offshoreward by current and diluted by mixing with the surrounding water. The case with the artificial beach is seen to be a little better than the case without it in offshoreward dispersion of fluorescent dye. It is because the offshore breakwaters serve as training walls against the

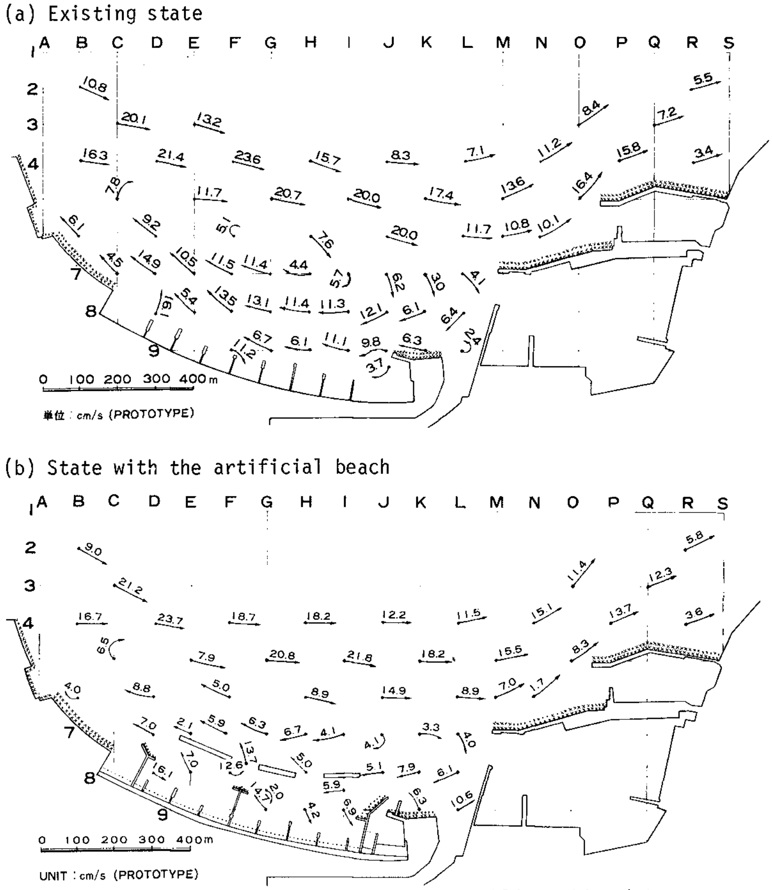

Fig. 19 Patterns of the fastest currents falling tide with summer swells

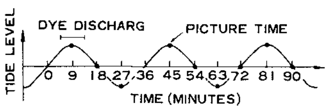

Fig. 20 Relation between tide and the time when dye-pictures were taken

current in their vicinity, as assumed from the current distribution in Fig. 19.

Model Test on Beach Evolution

For the model test on the evolution of artificial beach, in the model basin shown in Fig. 18, the area in the vicinity of the shore bounded with the dotted line was changed to the movable bed of fine sand of 0.17 mm in median diameter and the area deeper than 10 m deep was remolded to become constant depth of 10 m deep. Moreover, the wave generator was moved onto this part of constant depth and set to be parallel with the lattice wall. In this test, the water level was always M.W.L. and tidal currents was not generated.

Fig. 22 shows the changes of equi-depth lines due to wave action in the first proposed scheme. Model wave is 3 cm in height and 1 s in period which corresponds to the prototype wave of 3 m in height and 10 s in period by Floude's law. (a) and (b) in the figure corresponds respectively to before and after 3 hours of the run. As (b) is compared with (a), the foreshore near each groin of West and Center remarkably erodes and the area behind of each offshore breakwater remarkably accretes. Moreover, the mouth of the fishery basin in the eastside also shoals. As the countermeasures against such remarkable changes of the bottom topography, short wing breakwaters were attached at the tip or its vicinity of each groin and short jetty was added at the east side of the entrance of the fishery basin. Their effects are shown in Fig. 23, where the seawall is shifted seaward by 20 m in order to keep the space of the green belt and the windened road. Comparing this figure with Fig. 22, the changes of topography is much less remarkable. It means that the wing breakwater attached on the groin serves not only to prevent the erosion at the foot of the groin but also to restrain the accumulation behind the offshore-breakwater. The accumulation at the entrance of the fishery basin also has been moderated by the installation of the short jetty.

Change of Equi-Contour Lines at The Site

Construction of the West Offshore Breakwater has started in autumn of 1974, and its part of 120 m long has been completed until 1979. Fig. 24 shows the comparison of equi-contour lines between 1974 and 1979. Though the contour lines were in parallel with the shore-line in 1974, there are remarkable accumulation at the lee of the offshore breakwater in 1979. Especially the contour lines of ±0 and 2 m deep advance toward the offshore breakwater and the slope between 2 and 4 m deep is steeper than 1974. These tendency of sea-bed change in the lee of the offshore breakwater can be observed in the model test shown in Fig. 22 and 23, though the value of contour lines which changed remarkablly is a little different from the site. At the areas of the both side of the offshore breakwater, the area deeper than ±0 m are scoured, especially the contour lines of 1 to 3 m deep receding landwards. But, the contour lines higher than ±0 m deep do not recede on account of the exsistance of shore groins.

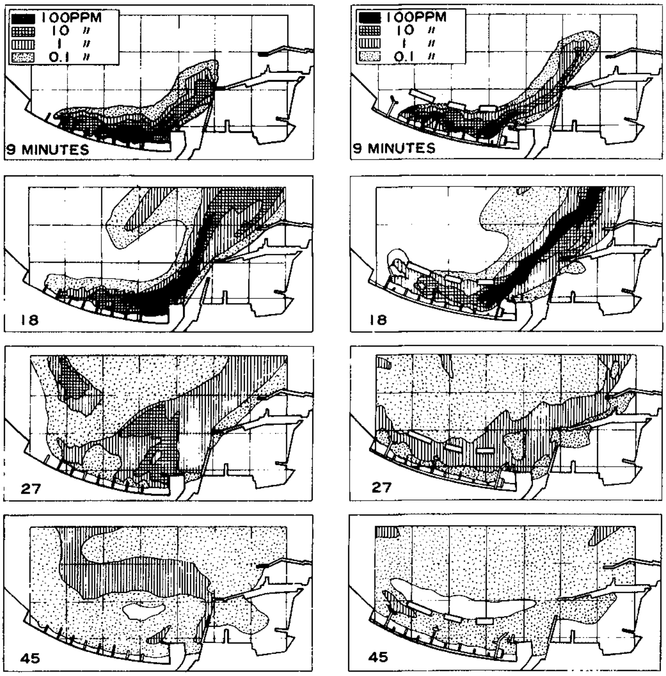

Fig. 21 Time change of dye dispersion

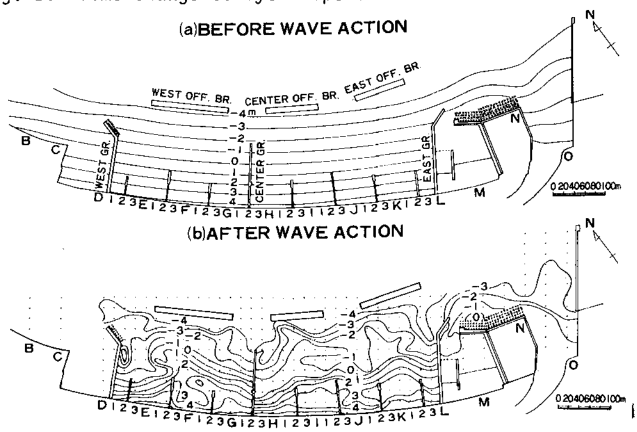

Fig. 22 Change of equi-depth line due to wave action for the first proposed scheme

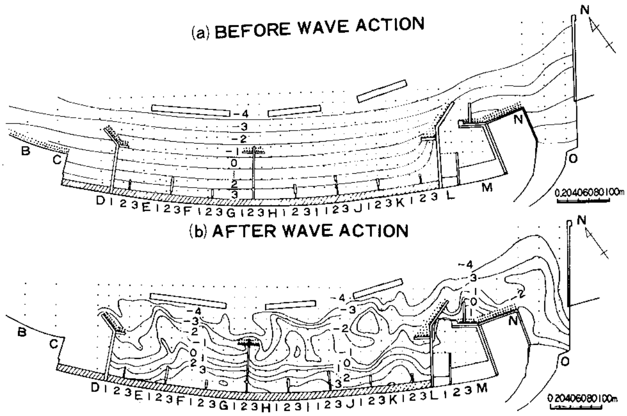

Fig. 23 Changes of equi-depth lines due to wave action for the artificial beach

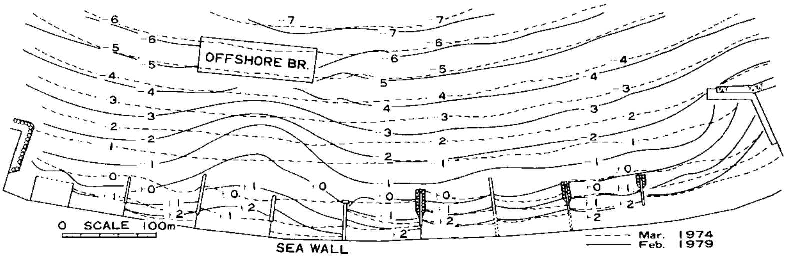

Fig. 24 Changes of equi-contour lines by the construction of west offshore breakwater at the site

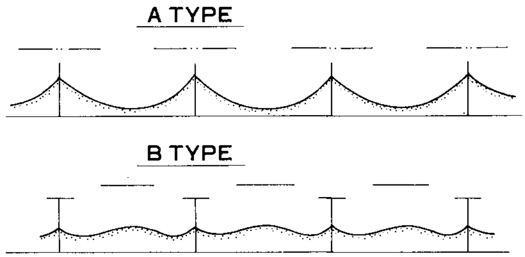

Fig. 25 Typical layouts of structures for the protection of an artificial beach

Conclusion

There are two types on the layout of the structures at artificial resort beach in Japan as shown in Fig. 25, one is the layout where a groin is installed behind an offshore breakwater as in Suma Beach and the other is the one where a groin is installed at the open part between offshore breakwaters as in Ito Beach. In the following description, the former layout is called A type and the latter one B type. The followings can be remarked from the above-mentioned tests:

(1) In A type layout, the shoreline of each compartment between groins is likely to change to concave one with recession at its center and advancement at its either side. The bottom-slope just in front of the foreshore becomes flatter in the middle part and steeper in the either side part. In this case, placement of a submerged breakwater near the foreshore in the middle of the compartment is not effective to prevent the recession of the middle part.

(2) In B type layout, the shoreline of each compartment tends to change to convex one with advancement at the center and recession at the either side. The bottom-slope of the middle part becomes steeper in the offshore far out of the foreshore though the part near the foreshore becomes flatter, and it of the either side becomes flatter in front of the foreshore.

(3) In A type layout, the groin must not be connected with the offshore breakwater from the stand-point of the prevention against the loss of the beach sand outwards of the offshore breakwater and the stagnation of polluted water in the inside of the offshore breakwater. Moreover, lowering the crown level of a little part in the center of the offshore breakwater serves to moderate the erosion at the middle part of the beach as well as the accumulation at the either side part of it.

(4) In B type layout, the groin should have a short wing breakwater at its tip. It serves to moderate the erosion near the groin as well as the accumulation behind the offshore breakwater.

ACKNOWLEDGEMENT

The authors express greatful thanks to the authorities of Kobe and Ito Cities for their presentation of many field data and to Messrs Hisao Kimura and Hideo Osanai in the same institute as the authors for their hearty cooperation in the model test.